PROCEEDINGS OF SCIENCE

Strained Superlattice photocathode development using CBE and MBE

Marcy Stutzman[a,*] Aaron Engel[b], and Chris Palmstrøm[b,c]

a Thomas Jefferson National Accelerator Facility,
12000 Jefferson Avenue, Newport News, VA 23606 USA

b Materials Department
University of California, Santa Barbara, Santa Barbara, CA 93106 USA

c Electrical and Computer Engineering
University of California, Santa Barbara, Santa Barbara, CA 93106 USA

E-mail: marcy@jlab.org, cjpalm@ucsb.edu

High polarization electron beams for accelerators are generated using strained superlattice GaAs-based photocathodes. A collaboration of researchers at University of California Santa Barbara and Jefferson Lab has been investigating growth of SSL photocathodes using either chemical- or molecular-beam epitaxy (CBE or MBE) to re-establish a source of high polarization photocathode material. While calibrating growth parameters for the most commonly used GaAs/GaAsP strained superlattice structure, the UCSB personnel encountered the drawbacks of growing structures with phosphorus in a MBE or CBE system, including high vapor pressure byproducts, phosphorus contamination in both the GaAs layer and all subsequent materials grown in that chamber, and highly flammable and toxic chamber residues.
For these reasons, the UCSB team began additionally investigating strained superlattices of InAlGaAs/AlGaAs, which has been successfully demonstrated in the literature[1], to be a high QE, high polarization photocathode material. For GaAs/GaAsP, varying phosphorus content affects both the band gap and polarization. However for InAlGaAs/AlGaAs, In and Al content can be varied independently and allows optimization of both polarization and bandgap.
Several variations on InAlGaAs/AlGaAs superlattice photocathodes, including those with distributed Bragg reflector (DBR) structures to enhance QE, have been grown at UCSB and sent to Jefferson Lab for testing. The initial results are quite promising, with polarization over 80% and QE about 0.3%, and ongoing test results will be presented.

25th International Spin Physics Symposium (SPIN 2023)
24-29 September 2023
Durham, NC, USA

[*] Speaker

© Copyright owned by the author(s) under the terms of the Creative Commons
Attribution-NonCommercial-NoDerivatives 4.0 International License (CC BY-NC-ND 4.0).

PoS(SPIN2023)215

1. Introduction

The US Department of Energy has prioritized restoring a reliable supply of high polarization photocathodes for the Nuclear and High Energy physics programs. High polarization photocathodes, are required for many experiments at Thomas Jefferson National Accelerator Facility (JLab), and will be required for a successful program at the Electron Ion Collider being constructed at Brookhaven National Lab. Strained Superlattice GaAs/GaAsP photocathode were developed and commercialized through a series of DOE SBIR funded projects, providing polarization greater than 85% and with about 1% QE, but the supplier no longer offers this material commercially.

We will present preliminary results of a collaborative project between JLab and the University of California Santa Barbara (UCSB) Materials Department investigating alternative growth techniques for GaAs/GaAsP phototocathodes, and the viability of InAlGaAs/AlGaAs photocathodes as an alternative to materials containing phosphorus, which is problematic in MBE growth chambers.

2. Polarized Photoemission

GaAs-based photocathodes were first used to generate polarized electron beams at accelerators in the 1970s [1]. GaAs is a direct band gap material, and is used as a spin polarized electron source by illuminating with circularly polarized light with energy just above the bandgap[2,3]. With proper surface preparation, unstrained GaAs photocathodes have a maximum electron beam polarization of 50%. To achieve higher polarization, GaAs layers are grown on a lattice mismatched substrate. The strain breaks a heavy-hole/light-hole degeneracy in the GaAs, giving a potential 100% polarized electron beam[4].

Strained superlattice structures have been developed to enhance the quantum efficiency (QE) while preserving strain and high polarization[5]. The thin layers preserve the strain of the emissive layers in the material, while having 15-20 layers of GaAs on GaAsP provides QE that is sufficient for accelerator operations.

3. GaAs/GaAsP SSL photocathodes

Superlattice GaAs/GaAsP photocathodes grown using MBE have been optimized through years of research[6], with the best wafers having QE over 1% and polarization around 90%. However, phosphorus in not commonly used in molecular beam epitaxy (MBE) or chemical beam epitaxy (CBE) growth chambers, optical constants for GaAsP compounds are less well characterized, and phosphorus leaves residue in the system that can cause memory effects in subsequent growths. Therefore, efforts have been ongoing to find GaAs based photocathode structures that maintain the high QE and polarization of GaAs/GaAsP but eliminate the difficulty of using phosphorus in MBE systems. Alternatives to GaAs/GaAsP, such as GaAsSb/AlGaAs, have been grown, but polarization has generally been lower than what the best GaAs/GaAsP photocathodes provide[6].

The UCSB/JLab project initially proposed using chemical beam epitaxy (CBE) instead of MBE for growing GaAs/GaAsP SSL materials. While MBE sources are typically elements

PoS(SPIN2023)215

evaporated at high temperatures, CBE growth can use vapor phase sources at lower temperatures, and the phosphorous would potentially be less problematic.

Preliminary calibration samples were grown using Triethyl gallium (TEGa) as the gaseous source for Ga in the structure, AsH_3 for arsenic and PH_3 for phosphorus. A graded layer test sample was grown, as shown in the reciprocal phase space map, which indicates the continuous change in lattice spacing from GaAs to GaAs(0.68)P(0.32), as seen in Figure 1. A second sample was grown to test superlattice growth parameters by growing GaAsP on GaAs. SIMS analysis shows sharp transitions between the layers indicating a high quality superlattice structure (see Figure 2). However, following these tests, the growth chamber had been contaminated with high vapor pressure byproducts of the TEGa and PH_3, and required substantial maintenance to recover the ability to grow anything without P contamination. This means that growing GaAsP using CBE does not offer advantages over the MBE or gas source MBE methods used by the previous supplier. Furthermore, using P in either MBE or CBE results in P contamination in other materials, and cannot be done in a multi-purpose deposition chamber where P contamination is unacceptable.

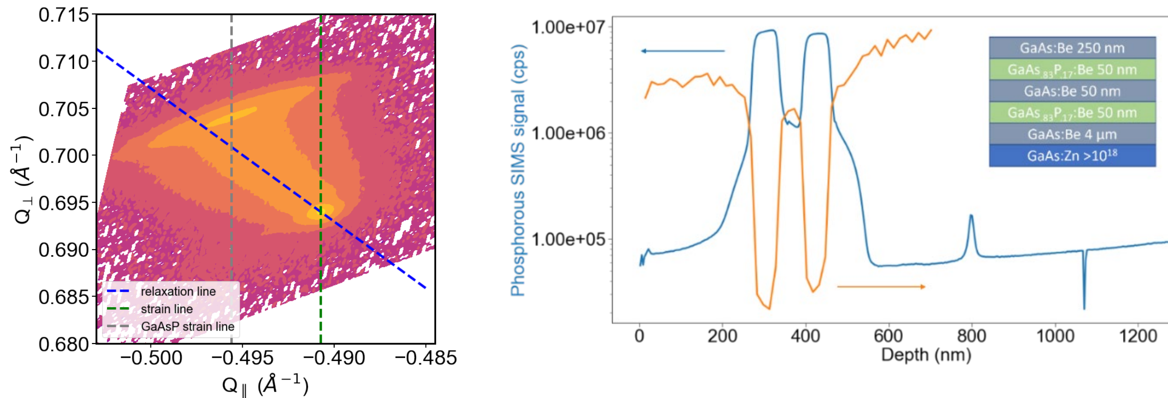

Figure 1: Reciprocal space mappiong of the lattice constant through the graded layer growth.

Figure 2: SIMS depth imaging of test superlattice structure showing sharp interfaces between GaAs and GaAsP layers.

With these growth issues evident for GaAs/GaAsP superlattice structures, a literature review found that InAlGaAs/AlGaAs superlattice structures had been successfully grown in St. Petersburg University [7] and tested at SLAC [8] . While the best wafer showed good polarization and QE, there was a good deal of variability in the performance between wafers. Therefore, we decided to pursue growing high polarization, high QE strained superlattices of InAlGaAs/AlGaAs using MBE, seeking to achieve the high polarization and sufficient QE of GaAs/GaAsP photocathodes.

4. InAlGaAs/AlGaAs SSL photocathodes

When growing InAlGaAs/AlGaAs photocathodes, the structure offers several advantages over GaAs/GaAsP photocathodes. In addition to the elimination of phosphorus, which is not desirable in MBE systems, the optimal growth temperatures for InAlGaAs and AlGaAs are similar, unlike GaAs and GaAsP. Furthermore, the quaternary structure of InAlGaAs/AlGaAs as the quantum well offers a higher degree of freedom in tailoring the strain and the wavelength

PoS(SPIN2023)215

independently. In Figure 3, $GaAs_xP_{1-x}$ can only be grown along the purple line, meaning that the lattice constant and the excitation energy are fixed: when growing $GaAs_{0.65}P_{0.35}$, the lattice parameter and bandgap cannot be varied independently. On the other hand, growing InAlGaAs/AlGaAs allows independent control of the strain and the bandgap. InAlGaAs can be grown with any ratio within the shaded aqua area. Furthermore, since the lattice constants for GaAs and AlAs are nearly identical, the bandgap of the well can be varied independent of the lattice parameters. The structures in the literature that were used as a first attempt at InAlGaAs/AlGaAs are shown with stars in Figure 3, with the composition $In_{0.16}Al_{0.23}Ga_{0.61}As/Al_{0.274}Ga_{0.726}As$.

PoS(SPIN2023)215

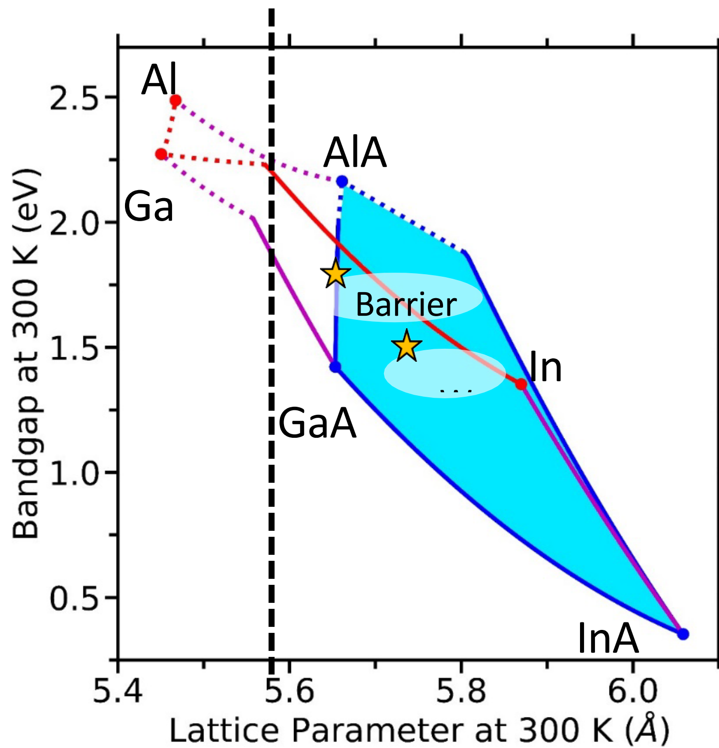

Figure 1: Map of lattice parameters and bandgaps used for wavelength engineering. Changing the GaAsP lattice constant necessitates a change in bandgap since the only allowable combinations are along the purple line. However, for InAlGaAs/AlGaAs, all states within the shaded area are allowed, so the lattice parameter, which affects strain, can be chosen, then the bandgap independently adjusted to optimize the photoemission wavelength. Additionally, the lattice parameters for both GaAs and AlGaAs are nearly identical so that a virtual substrate is not required.

Finally, the AlGaAs barrier has a lattice constant nearly identical to the GaAs substrate, so AlGaAs can be grown directly on GaAs, or a GaAs/AlGaAs substrate can transition from the GaAs to AlGaAs without the need to grow a thick transition layer to a GaAsP virtual substrate. This will enable InAlGaAs/AlGaAs photocathodes to be grown considerably more quickly and with less cost. By eliminating the graded layer and virtual substrate, lattice dislocations and strain relaxation effects are minimized, which can lead to higher quality films and the reduction of charge asymmetry effects with the reversal of helicity of the excitation light. The structures for GaAs/GaAsP and InAlGaAs/AlGaAs are shown in Figure 4 adjacent to one another and roughly to scale.

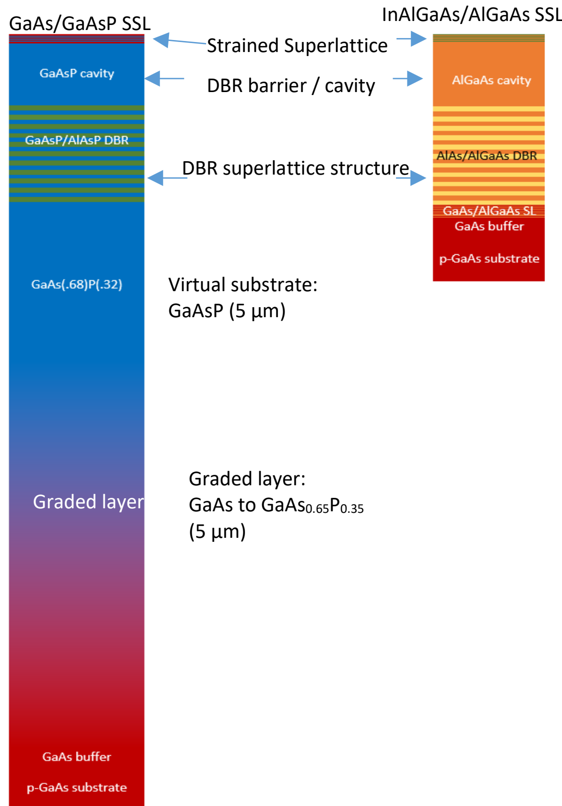

Figure 2: The structures for GaAs/GaAsP and InAlGaAs/AlGaAs. Both have the top superlattice layers, the cavity for the DBR and the DBR depth comparable. For the GaAsP, a graded layer must be grown on the GaAs substrate to smoothly vary from the GaAs lattice constant to the $GaAs_{0.65}P_{0.35}$ lattice constant, which is a slow and expensive process, and leads to dislocations propogating to the surface. The InAlGaAs/AlGaAs on the other hand needs only a thin superlattice layer to transition between the substrate and either the barrier layer or the DBR layer due to the well matched lattice constants.

4.1 InAlGaAs/AlGaAs and Distributed Bragg Reflectors

Another advantage of the InAlGaAs/AlGaAs structure is compatibility with a distributed Bragg Reflector (DBR) structure in the growth. DBR structures are grown by making a layer that reflects the incident light back through the photoemissive layer several times which can enhancing QE while maintaining polarization[9]. The optical properties of AlAs and AlGaAs, which are used as a DBR for InAlGaAs/AlGaAs, are well known and the deposition temperatures are compatible with the rest of the structure. Alternately, for GaAs/GaAsP, the DBR is made using GaAsP and AlAsP, and the optical characteristics and deposition temperatures of the phosphorous layers are less well characterized and more difficult to grow.

A preliminary study of growing a DBR structure was performed at UCSB, with 12 periods of AlGaAs (57 nm) grown on AlAs (65 nm) to calibrate growth rates and peak wavelength calculations. This first test sample had a peak reflectivity at 755 nm rather than the designed 780 nm (see Figure 5), and the feedback from this will be used to tune future DBR photocathodes. , Uniformity was relatively consistent across the sample, with less than 10 nm variation in the peak between the center and edges, and this can be improved by rotating the sample during deposition when full photocathode structures are grown in the future.

PoS(SPIN2018)

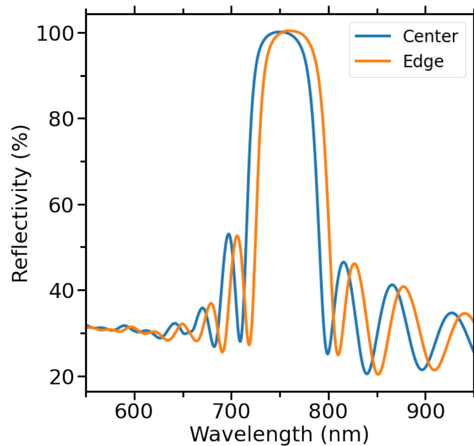

Figure 3: Reflectivity vs. wavelength for a calibration of DBR structure growth. The peak wavelength was offset from the designed 780 nm, but had a broad 50 nm bandwidth for high reflectivity.

5. Experimental Results

5.1 Photoluminescence

Six samples were fabricated at UCSB and sent for testing at Jefferson Lab. The first three differed in the growth temperatures. Photoluminescence studies of samples grown at 560, 520 and 480 °C are shown in Figure 6. The figure shows the data, with peaks evident between 1.6 and 1.7 eV (corresponding to ~700 and 800 nm). A larger integrated intensity can be due to enhanced absorption of light or enhanced recombination of electron-hole pairs in the superlattice, indicating that lower growth temperatures will produced photocathodes with higher quantum efficiency.

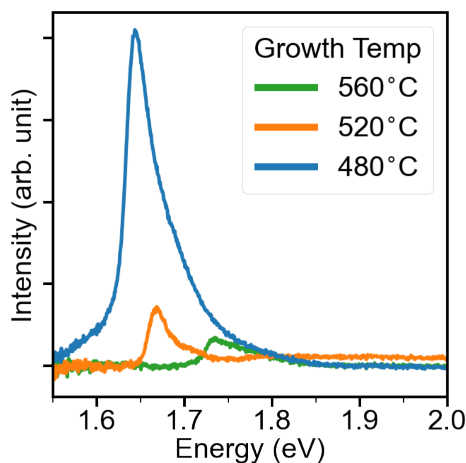

Figure 4: Photoluminescence (PL) studies showing the optical properties of the structures. The enhancement of the photoluminescence peak in this background subtracted image indicates a potential for improvement in QE with lower growth temperatures.

PoS(SPIN2023)215

5.1 X-ray diffraction

These same three samples were also studied using x-ray diffraction, which measures the interface quality, the period of the superlattice, and the average out-of-plane lattice constant of a superlattice period. The sample grown at 480°C shows more fringes in the XRD trace, which indicates that the lower growth temperature has led to sharper interfaces in the strained superlattice structure, as seen in Figure 7.

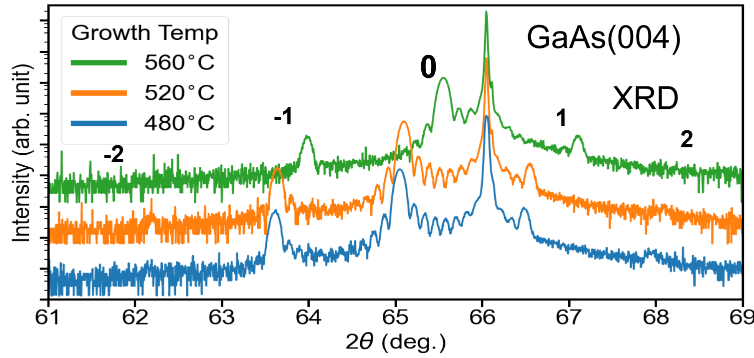

Figure 5: The XRD peaks become sharper with the lower growth temperatures, indicating better structural quality and sharper interfaces as the growth temperaturer decreases.

5.3 Random Alloy Disorder

By using a quaternary well (InAlGaAs) and a tertiary barrier (AlGaAs), the structure can be customized and optimized as discussed above. However, these layers can suffer from effects from random alloy disorder, where atomic scale variations can affect the electron excitation and transport. This could reduce the heavy hole/light hole splitting due to the strained barrier, or the energy levels for the heavy and light holes could broaden, which would decrease the maximum polarization.

A growth technique known as digital alloying[10] can be used to alleviate random alloy disorder effects. A digital alloy uses thin layers of the components of a layer; for instance, instead of growing $Al_{0.33}Ga_{0.67}As$ for the barrier, a layered structure of AlAs and GaAs with the thickness ratio of 1:2 to achieve the desired stoichiometry. For a structure of $In_{0.16}Al_{0.23}Ga_{0.61}As$, the digital alloy illustrated in Figure 8 can be used to get the proper In to Al ratio.

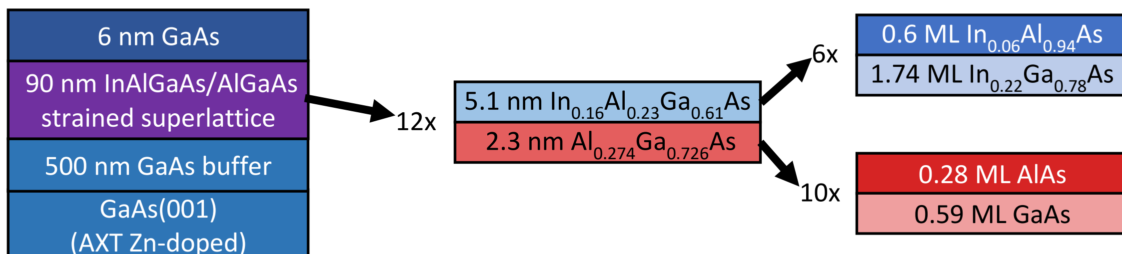

Figure 6: Digital alloy growth to reduce effects due random alloy disorder. The tertiary and quatenary structures can vary in composition spatially, so changing to a digital alloy with fewer elements in each layer can make the distribution of the alloy more uniform. One sample with a digital barrier has been grown and sent to JLab, and is awaiting testing.

PoS(SPIN2023)215

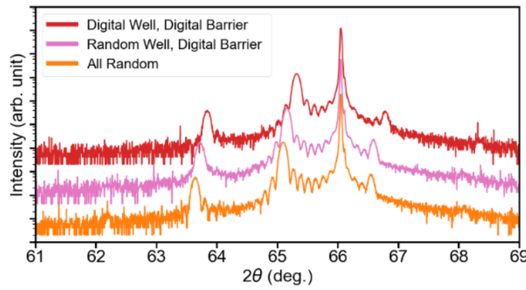

Figure 9: XRD studies of digital alloy samples. The lack of additional peaks in the digital barrier or well indicate that the superlattice layers are not sharp layers.

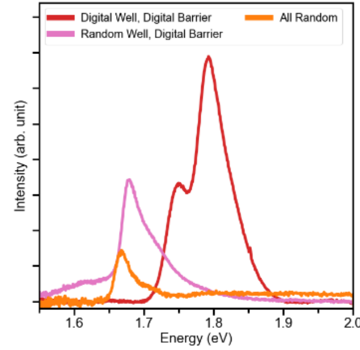

Figure 10: Photoluminescence studies show an increase in the sharpness of the PL peaks with the addition of a digital barrier or both a digital well and digital barrier

Several samples of digital alloy were grown and characterized using XRD and photoluminescence, as shown in Figures 9 and 10. For these tests, the samples were not doped, so they are suitable for characterization but not for use as photocathodes. The XRD peaks showed no significant difference between the all digital, part digital and all random alloy, though the PL peak was strongest for the all digital structure. One sample with digital barriers has been sent to Jefferson Lab for testing and is awaiting evaluation.

6. Photocathode evaluation

Six photocathode were sent for evaluation in the Jefferson Lab retarding field Mott polarimeter[11]. The fires UCSB sample was measured in the fall of 2022. The polarimeter then experienced several failures due to aging components, and a change in the detector design introduced a new requirement for mounting the channel electron multiplier detectors. The polarimeter was returned to service in fall of 2023, and measurements of further samples are in progress.

The polarization and quantum efficiency from the first UCSB sample are shown in Figure 11. Maximum polarization is about 80% with QE of 0.2% at the maximum polarization wavelength. While this initial result is promising, the separation between the heavy hole 1 band and the light hole 1 band, indicated by black boxes in Figure 11, is approximately 50 meV compared to near 100 meV for GaAs/GaAsP. This could be a consequence of the random alloy disorder, and a digital alloy sample is awaiting testing to determine if the digital alloy can increase the separation of these bands.

PoS(SPIN2023)215

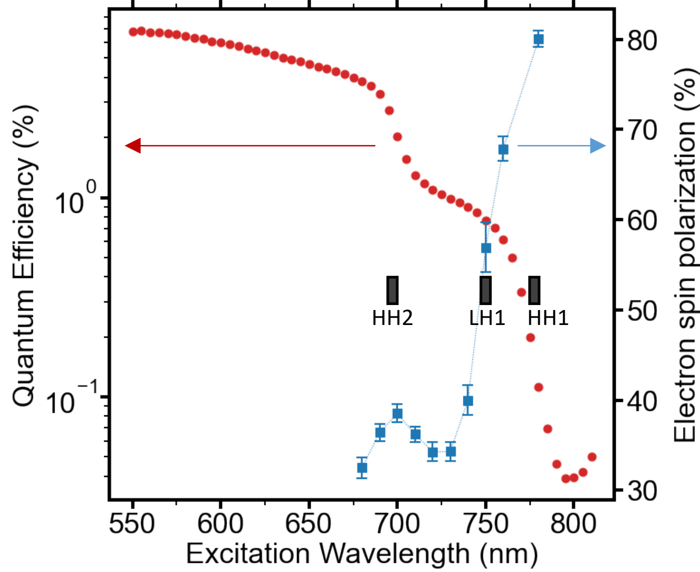

Figure 7: QE and polarization for UCSB sample 1. The energies for heavy hole and light hole excitation are approximated with the black boxes: Over 780 nm, only electrons from the heavy hole 1 band are excited, giving maximum polarization. By 750 nm, a significant fraction of the photoemission is from the light hole 1 band, and by 700 nm, electrons are being promoted from the heavy hole 2 band as well with considerably lower polarization.

7. Conclusions

The use of Chemical Beam Epitaxy as an alternative to Molecular Beam Epitaxy to grow GaAs/GaAsP high polarization photocathodes demonstrated that a gaseous Ga source is undesirable in the growth process due to its high vapor pressure byproducts with used with phosphine gas. With phosphorus problematic in MBE systems, the project pivoted to studying InAlGaAs/AlGaAs SSL photocathodes.

A series of InAlGaAs/AlGaAs photocathodes were grown at different growth temperatures, different lattice parameters and layer thicknesses to increase polarization, and with digital alloys to reduce effects from random alloy disorder. InAlGaAs/AlGaAs has benefits over GaAs/GaAsP from a growth standpoint, including more compatible temperatures between the superlattice layers, less problematic growth byproducts, and the ability to use a subset of the high polarization SSL sources for the distributed Bragg reflector superlattice.

The samples were tested at UCSB using x-ray diffraction and photoluminescence. In the PL analysis, lower growth temperatures and all-digital alloys corresponded with sharper PL peaks. In the XRD analysis, the lower growth temperatures also showed better XRD fringes indicating sharper interfaces, though there were not significant differences between digital-alloy and all-random structures in the XRD patterns.

The first sample was evaluated at JLab using the retarding field Mott polarimeter, and yielded polarization about 80% and QE about 0.2%. The JLab polarimeter has been repaired, and the rest of the samples are currently being tested.

PoS(SPIN2023)215

Acknowledgements

This work is supported by funding from the US DOE FOA LAB 20-2310.
This material is based upon work supported by the U.S. Department of Energy, Office of Science, Office of Nuclear Physics under contract DE-AC05-06OR23177.

References

[1] C.Y. Prescott et al., *Parity non-conservation in inelastic electron scattering*, Physics Letters B **77,** p. 347, (1978). https://doi.org/10.1016/0370-2693(78)90722-0

[2] D.T. Pierce et al., *The GaAs spin polarized electron source,* Rev. Sci. Instrum. **51,** p.478 (1980). https://doi.org/10.1063/1.1136250

[3] Wei Liu, M. Poelker, X. Peng, S. Zhang and M.L. Stutzman, A comprehensive evaluation of factors that influence the spin polarization of electrons emitted from bulk GaAs photocathodes, J. Applied Physics, **122**, p. 035703, (2017). https://doi.org/10.1063/1.4994306

[4] T. Maruyama et al., *Electron-spin polarization in photoemission from strained GaAs grown on* $GaAs_{1-x}P_x$, Phys. Rev. B, 46 (1992) 4261. https://doi.org/10.1103/PhysRevB.46.4261

[5] T. Maruyama et al., Systematic study of polarized electron emission from strained GaAs/GaAsP superlattice photocathodes, Appl.Phys.Lett. **85** 2640 (2004). https://doi.org/10.1063/1.1795358

[6] Wei Liu, Y. Chen, A.Moy, M. Poelker, M.L. Stutzman, S. Zhang, *Evaluation of GaAsSb/AlGaAs strained superlattice photocathodes*. AIP Advances **8**, 075308 (2018). https://doi.org/10.1063/1.5040593

[7] L.G. Gerchikov, Yu.A. Mamaev et al., “Photoemission of Polarized Electrons from InAlGaAs/GaAs Superlattices with Minimum Conduction Band Offsets”, Semiconductors (2006) **40** p. 1326. https://doi.org/10.1134/S1063782606110133

[8] Yu.A. Mamaev, A. Subashiev, Yu. Yashin, L. Gerchikov, T. Maruyama, D.-A Luh, J. Clendenin, V. Ustinov, A. Zhukov, *InAlGaAs/AlGaAs Superlattices for Polarized Electron Photocathodes.* SLAC-PUB-11403 August, 2005. doi:10.2172/839712.

[9] Wei Liu, Y. Chen, W. Lu, A. Moy, M. Poelker, M.L. Stutzman, S. Zhang *Record-level quantum efficiency from a high polarization strained GaAs/GaAsP superlattice photocathode with distributed Bragg reflector* Appl. Phys. Lett. **109**, 252104 (2016); https://doi.org/10.1063/1.4972180

[10] J. D. Song, W. J. Choi, J. M. Kim, K. S. Chang, Y. T. Lee*, MBE growth and optical properties of digital-alloy 1.55μm multi-quantum wells*, Journal of Crystal Growth, Volume **270** (2004), p295. https://doi.org/10.1016/j.jcrysgro.2004.06.037

[11] J.L. McCarter, M.L. Stutzman, K.W. Trantham, T.G. Anderson, A.M. Cook, T.J. Gay, *A low-voltage retarding-field Mott polarimeter for photocathode characterization.* Nucl. Instr. and Meth., A618 (2010) 30. doi.org/10.1016/j.nima.2010.02.123

PoS(SPIN2023)215